

Identification and characterization of murine adipose tissue-derived somatic stem cells of Shenque (CV8) acupoint

Yu-Hui Hao^{1,2}, Zhi-Zhen Liu¹, Hong Zhao¹, Lei Wang¹, Ajab Khan¹, Jian-Bin Mu³, Yu-Fei Wang¹, Li-Hong Yang¹, Ran Zhou⁴, Jun Xie¹

¹Shanxi Key Laboratory of Birth Defect and Cell Regeneration, Shanxi Medical University, Taiyuan, Shanxi 030001, China;

²Department of Basic Medicine, Xinzhou Vocational and Technical College, Xinzhou, Shanxi 034000, China;

³Laboratory of Malaria and Vector Research, National Institute of Allergy and Infectious Diseases, National Institutes of Health, Bethesda, MA 20852, USA;

⁴Basic Medical College, Shanxi University of Chinese Medicine, Jinzhong, Shanxi 030619, China.

Abstract

Background: Shenque (CV8) acupoint is located on the navel and has been therapeutically used for more than 2000 years in Traditional Chinese Medicine (TCM). However, clinical research on the underlying therapeutic molecular mechanisms of the CV8 acupoint lags far behind. This study aimed to study the mechanisms of umbilical acupoint therapy by using stem cells.

Methods: The morphological characteristics of CV8 acupoint were detected under a stereomicroscope using hematoxylin and eosin (H&E) staining. Oil Red, Masson, and immunohistochemical staining on multi-layered slices were used to identify the type of cells at the CV8 acupoint. Cell proliferation was measured by a cell counting kit-8 (CCK-8) method. Flow cytometry and immunohistochemistry were used for cell identification. Induced differentiation was used to compare the differentiation of cells derived from CV8 acupoint and non-acupoint somatic stem cells into other cell types, such as osteogenic, adipogenic, and neural stem cell-like cells.

Results: Morphological observations showed that adipose tissues at the linea alba of the CV8 acupoint in mice had a mass-like distribution. Immunohistochemical staining confirmed the distribution of stem cell antigen-1 (Sca-1) positive cells in the multi-layered slices of CV8 acupoint tissues. Cells isolated from adipose tissues at the CV8 acupoint exhibited high expression of Sca-1 and CD44 and low expression of CD31 and CD34, and these cells possessed osteogenic, adipogenic, and neurogenic stem cell-like cell differentiation ability. The cell proliferation (day 4: 0.5138 ± 0.0111 vs. 0.4107 ± 0.0180 , $t = 8.447$, $P = 0.0011$; day 5: 0.6890 ± 0.0070 vs. 0.5520 ± 0.0118 , $t = 17.310$, $P < 0.0001$; day 6: 0.7320 ± 0.0090 vs. 0.6157 ± 0.0123 , $t = 13.190$, $P = 0.0002$; and day 7: 0.7550 ± 0.0050 vs. 0.6313 ± 0.0051 , $t = 42.560$, $P < 0.0001$), adipogenic (9.224 ± 0.345 % vs. 3.933 ± 1.800 %, $t = 5.000$, $P = 0.0075$), and neurogenic stem cell-like cell differentiation (diameter $< 50 \mu\text{m}$: 7.2000 ± 1.3040 vs. 2.6000 ± 0.5477 , $t = 7.273$, $P < 0.0001$; diameter $50\text{--}100 \mu\text{m}$: 2.6000 ± 0.5477 vs. 1.0000 ± 0.7071 , $t = 4.000$, $P = 0.0039$; and diameter $> 100 \mu\text{m}$: 2.6000 ± 0.5477 vs. 0.8000 ± 0.8367 , $t = 4.025$, $P = 0.0038$) were significantly enhanced in somatic stem cells derived from the CV8 acupoint compared to somatic stem cells from the groin non-acupoint. However, cells possessed significantly weaker osteogenicity (2.697 ± 0.627 % vs. 7.254 ± 0.958 %, $t = 6.893$, $P = 0.0023$) in the CV8 acupoint group.

Conclusions: Our study showed that CV8 acupoint was rich with adipose tissues that contained abundant somatic stem cells. The biological examination of somatic stem cells derived from the CV8 acupoint provided novel insights for future research on the mechanisms of umbilical therapy.

Keywords: Shenque (CV8) acupoint; Non-acupoint site; Navel; Adipose tissue; Somatic stem cells; Stem cell antigen-1 (Sca-1); Umbilical therapy

Introduction

Acupoints are essential sites on the body's surface, where qi and blood aggregate and support the body functions, and are studied in Traditional Chinese Medicine (TCM). Acupoints are connected to tissues and organs through meridians that reflect their physiological or pathological

conditions.^[1] In addition, acupoints are sites for acupuncture, massage, and other external treatments. The uses of acupoints to treat diseases have lasted for thousands of years in TCM, but the way how acupoints elicit their effects is still an unsolved mystery.

Compared with non-acupoint sites, acupoints have high electrical conductivity that is supposed to be associated

Access this article online

Quick Response Code:



Website:

www.cmj.org

DOI:

10.1097/CM9.0000000000001850

Correspondence to: Prof. Jun Xie, Shanxi Key Laboratory of Birth Defect and Cell Regeneration, Shanxi Medical University, Taiyuan, Shanxi 030001, China
E-Mail: junxie@sxmu.edu.cn

Copyright © 2021 The Chinese Medical Association, produced by Wolters Kluwer, Inc. under the CC-BY-NC-ND license. This is an open access article distributed under the terms of the Creative Commons Attribution-Non Commercial-No Derivatives License 4.0 (CCBY-NC-ND), where it is permissible to download and share the work provided it is properly cited. The work cannot be changed in any way or used commercially without permission from the journal.

Chinese Medical Journal 2021;134(22)

Received: 13-01-2021 Edited by: Pei-Fang Wei

with the denser dermal papillae in acupoints that are rich in sympathetic nerve fibers.^[2,3] A hypothesis “blood vessel-nerve bundle penetrating the superficial fascia” was proposed by a researcher through histological observations of Shenmen and Zusanli acupoints.^[4] Laser scanning confocal microscopy and immunohistochemistry observation reveal that dermal layers of the Zhongwan acupoint in rabbits contain unique catecholamine-storing cells.^[5] Acupoints in microvascular beds are rich in blood supply. Blood flow spectral analysis reveals that the difference between acupoint and non-acupoint microcirculation is due to the myogenic reaction of vascular beds.^[6] Electrical resistance for the lung channel using Lieque and Taiyuan acupoints showed that the skin electrical resistance in patients with asthma is significantly higher than that of the healthy subjects.^[7] She *et al*^[8] observed blood vessels, mast cells, and acetyl cholinesterase-responsive nerves at acupoint tissues and showed that electro-acupuncture results in mast cell recruitment and migration along the blood vessels and nerve bundles.

TCM works on the Shenque (CV8) acupoint that is anatomically located at the navel to treat diseases for more than 2000 years. Studies on the CV8 acupoint to elicit its effects in navel therapy are currently focused on the role of mast cells. Navel therapy to treat a dysmenorrhea rat model induced an increased number of mast cells in the CV8 acupoint and promoted their degranulation to achieve the therapeutic effects.^[9] Indirect moxibustion cones to treat a rat model of irritable bowel syndrome associated with diarrhea (IBS-D) result in mast cell activation.^[10] Therefore, it was hypothesized that mast cells might be one of the important factors in the amplification of biological signals during IBS-D treatment using indirect moxibustion cones. However, the exact mechanism of umbilical acupoint therapy remains to be elucidated.

In the TCM theory, the umbilicus is regarded as the source of five solid and six hollow organs and the root of promordial qi. CV8 acupoint is believed to regulate the normal physiological activity of organs and meridians.^[11] Promordial qi is considered as the “earliest material” in TCM but with no links to any cell types or tissues to date. However, in modern medicine, stem cells are considered as the building blocks for tissues and cells in the human body and with the ability to self-renew and differentiate into tissue-specific cells. These abilities allow stem cells to participate in self-repair and self-renewal of tissues and cells, immune regulation, and so on.^[12] In addition, increasing evidence has shown that when somatic stem cells are in a new microenvironment, they can differentiate into other types of cells to exert their functions.

Although the theoretical framework of TCM differs from modern medicine, the function of CV8 acupoint in the TCM theory is somewhat similar to the function of somatic stem cells in modern medicinal theory. We therefore examined, for the first time, the possible association between the adipose tissue at CV8 acupoint and the somatic stem cells. We further explored the effects of the stem cells derived from the CV8 acupoint and non-acupoint site. Our study aimed to provide novel experimental methods and research

insights for studying the mechanisms of umbilical acupoint therapy using stem cells.

Methods

Experimental animals

Fifty specific pathogen-free (SPF)-grade Balb/c mice (4–16-week-old) were provided by the Animal Center of Shanxi Medical University. All animal handling procedures were performed in accordance with the National Institute of Health “Guidelines on the Use of Laboratory Animals” (publication No. 85–23, revised in 1996) and were approved by the Shanxi Medical University Committee of Animal Care (No. SYXK[Jin]2019–0007).

Materials

Materials used in this study were listed as follows: Dulbecco’s modified eagle medium (DMEM)-low glucose (HyClone, Logan, UT, USA); DMEM/F12 culture medium (HyClone); B27 supplement without vitamin A (Gibco, New York, NY, USA); recombinant murine epidermal growth factor (EGF) (PeproTech, Rocky Hill, NJ, USA); recombinant murine fibroblast growth factor (FGF)-basic (PeproTech); 0.5% Oil Red O solution (Solarbio, Beijing, China); Masson Stain Kit (Nanjing Jiancheng Technology Co., Ltd., Nanjing, Jiangsu, China); cell proliferation assay kit (KeyGen Biotech Co., Ltd., Nanjing, Jiangsu, China); mouse osteogenesis induction and differentiation base media and mouse adipogenesis induction and differentiation base media (Cyagen Biosciences Co., Ltd., Guangzhou, Guangdong, China); anti-mouse Ly-6A/E (stem cell antigen-1, Sca-1) phycoerythrin (PE), anti-mouse CD34 fluorescein isothiocyanate (FITC), anti-mouse CD31 (platelet endothelial cell adhesion molecule-1, PECAM-1) FITC, anti-human/mouse CD44 PE (eBioscience, San Diego, CA, USA); anti-nestin antibody, goat anti-mouse immunoglobulin G (IgG)-FITC (Santa Cruz Biotechnology, Inc., Santa Cruz, CA, USA); goat anti-mouse IgG (H+L)-horseradish peroxidase (HRP) (Jackson ImmunoResearch, West Grove, PA, USA); and Alizarin Red S solution (Solarbio, Beijing, China).

Hematoxylin and eosin (H&E), Oil Red O, and Masson staining

Old Balb/c mice of 4 weeks, 8 weeks, 12 weeks, and 16 weeks (five males and five females in each group) were selected to observe the general morphology of the CV8 acupoint. The females and males were weighed 17.4 ± 1.38 g and 18.1 ± 1.62 g, respectively. The slices were fixed in 10% formalin, paraffin-embedded, and stained with H&E. Oil Red O and Masson staining was carried out according to the manufacturer’s instructions.

Immunohistochemical staining

Anti-Sca-1/Ly6A/E antibody (Abcam, Cambridge, UK) with a 1:100 dilution and goat anti-mouse IgG (H+L)-HRP (Jackson ImmunoResearch) with a 1:500 dilution were used as primary antibody and secondary antibody, respectively. The staining procedure was carried out according to the manufacturer’s instructions (Abcam).

Isolation and culture of cells

Ten SPF-grade female BALB/c mice (16-week-old) weighing 28 to 30 g were purchased. The mice were euthanized using cervical dislocation. Adipose tissues from the CV8 acupoint and non-acupoint sites in the groin were isolated, washed multiple times with phosphate-buffered saline (PBS) containing dual antibiotics (penicillin and streptomycin), and placed in 2-mL Eppendorf (EP) tubes with several drops of culture medium. The ophthalmology scissors were used to cut the tissues into 1 mm × 1 mm × 1 mm blocks in 6-well culture plates. A low glucose culture medium containing 10% fetal bovine serum (FBS) was added to the culture plates and was incubated in a 37°C and 5% CO₂ cell culture incubator. Cells isolated from adipose tissues derived from the CV8 acupoint and the groin non-acupoint adipose tissues were considered to be experimental and control groups, respectively.

Flow cytometry cell analysis

Healthy P3 somatic stem cells from the CV8 acupoint and groin non-acupoint were re-suspended and loaded into flow cytometry tubes. In the first tube, anti-mouse IgG PE and anti-mouse IgG FITC were added; in the second tube, anti-mouse Ly-6A/E (Sca-1) PE and anti-mouse CD31 FITC were added; and in the third tube, anti-mouse CD44 PE and anti-mouse CD34 FITC were added. The tubes were incubated in the dark at a room temperature for 30 minutes. The excess antibodies were washed away, followed by centrifugation, re-suspension, and flow cytometry.

Cell counting kit-8 (CCK-8) method

Using a hemocytometer, healthy P3 somatic stem cells from the CV8 acupoint and groin non-acupoint were counted, and 2500 cells per well were inoculated in a 96-well plate. The assay was carried out according to the manufacturer's instructions (KeyGen Biotech Co., Ltd.), and values were recorded for seven consecutive days. A growth curve of cells was plotted against time on the horizontal axis and absorbance on the vertical axis.

Adipogenic differentiation, identification, and comparison

Healthy P3 somatic stem cells from the CV8 acupoint and groin non-acupoint were re-suspended and inoculated in 6-well plates at a density of $2 \times 10^4/\text{cm}^2$ for adipogenic induction following the manufacturer's instructions (Cyagen Biosciences Co., Ltd.). The presence of fat droplets was observed and photographed after Oil Red O staining. The adipogenic differentiation between the CV8 acupoint and non-acupoint site was analyzed by calculating the percentage of Oil Red O stained area using ImageProPlus 6.0 (Media Cybernetics, Rockville, MD, USA) software.

Osteogenic differentiation, identification, and comparison

Healthy P3 somatic stem cells from CV8 acupoint and non-acupoint sites were re-suspended and inoculated in 6-well plates at a density of $3 \times 10^3/\text{cm}^2$ and then the procedures followed the manufacturer's instructions

(Cyagen Biosciences Co., Ltd.). After 4 weeks of differentiation, the cells were fixed and stained with Alizarin Red S. The presence of mineralized nodules was observed in five different microscopic fields for comparing osteogenic differentiation between both groups. The images were analyzed with ImageProPlus 6.0 (Media Cybernetics, Rockville, MD, USA) software, and the following formula was used to calculate the percentage of mineralization: area of mineralized nodules/field area × 100%.

Neurogenic stem cell-like cells differentiation, identification, and comparison

Healthy P3 somatic stem cells from the CV8 acupoint and non-acupoint sites were re-suspended in DMEM/F12 culture medium containing B27, EGF, and basic fibroblast growth factor (bFGF) followed by inoculation into 6-well plates at a density of $2 \times 10^5/2.5$ mL. The cells were observed and photographed every day for morphological changes. After the cells formed clumps in the 6-well plates and differentiated into neural stem cell-like cells (which grew similar to neurospheres), these were inoculated onto glass slides containing poly-L-lysine. After 3 hours, the glass slides were removed, and the immunofluorescence assay was carried out using 1:20 anti-nestin antibodies as primary antibodies and 1:100 goat anti-mouse IgG-FITC as secondary antibodies to identify neural stem cells. Image data were analyzed using Image-J software (National Institutes of Health, Bethesda, MD, USA), and nerve spheres were counted from five randomly selected visual fields of each group (diameter <50 μm; diameter 50–100 μm; and diameter >100 μm).

Statistical analysis

The continuous data with normal distribution were expressed as mean ± standard deviation. Intergroup comparison was carried out using a *t* test. The SPSS 22.0 (SPSS Inc., Chicago, IL, USA) statistics software was used for analysis, and the test level was $\alpha = 0.05$. A value of $P < 0.05$ was considered to be statistically significant. The Graph Pad Prism5 software (GraphPad Software Inc., San Diego, CA, USA) was used to plot statistical graphs.

Results

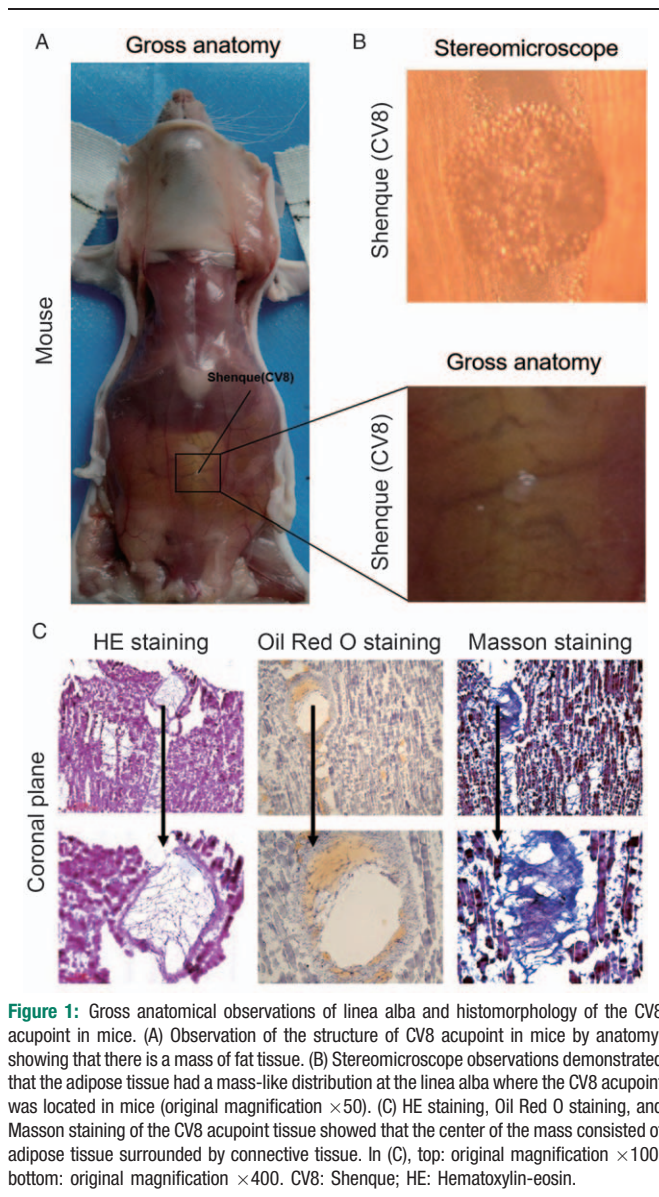
Gross anatomical observations of linea alba at the CV8 acupoint

The anatomical location of the CV8 acupoint was determined according to the meridian and acupoint map of mice and it is located at the navel in the linea alba.^[13] Gross observation at the anatomical location of the CV8 acupoint showed that there was a patch-like distribution of adipose tissues at the linea alba [Figure 1A]. Further observation under the stereomicroscope showed that adipose tissues formed a ball-like fat mass [Figure 1B].

Histomorphological observations of the CV8 acupoint

Tissues from the CV8 acupoint were isolated for H&E staining of coronal sections. The center of the navel in mice was observed to be composed of tissues that were Oil Red

O-positive and rich in adipose cells. This region was also positive for Masson staining, and connective tissue was observed around the adipose cells [Figure 1C].



Sca-1 immunohistochemical staining of CV8 acupoint tissues

Tissues from the CV8 acupoint in mice were extracted and divided into multiple continuous cross sections. Sca-1 was used as a primary antibody, and anti-mouse IgG (H+L)-HRP was used as a secondary antibody for immunohistochemical staining. Results showed that various sections in the CV8 acupoint contained Sca-1-positive cells [Figure 2].

Morphology and immunophenotyping of somatic stem cells from the CV8 acupoint and groin non-acupoint

When adherence culture was carried out for 3 days on tissue blocks, cells were detached from the tissue blocks of both groups (somatic stem cells from the CV8 acupoint and groin non-acupoint) and adhered to the walls of culture plates. After 7–10 days of inoculation, the adherent cells were approximately 80% confluent. Subsequently, the cells were equally passaged after every 4 days. The P1 cells of both groups showed diverse short fusiform, triangular, and polygonal morphology. After passaging to P3, cells of both groups were observed to have a similar long fusiform and fibroblast-like morphology. The cells exhibited a single morphology and an eddy-like growth pattern [Figure 3A]. The flow cytometry results showed high expression of stem cell markers, Sca-1 and CD44, and low expression of CD31 and CD34 in both groups [Figure 3B].

Comparison of proliferation ability of somatic stem cells from two acupoints

The CCK-8 method was used to detect cell proliferation characteristics of the two groups. Both groups showed an S-shaped proliferation growth curve. At the first 72 hours, cell growth was slow. After 72 hours, the cells entered the logarithmic growth phase, and cell proliferation was significantly accelerated. The logarithmic phase lasted from day 3 to 5. From day 5 to day 7, cell proliferation started to decrease and entered the plateau phase that was consistent with the *in vitro* cell proliferation. However, from day 4, the proliferation rate of the CV8 acupoint group was significantly higher than the groin non-acupoint (day 4: 0.5138 ± 0.0111 vs. 0.4107 ± 0.0180 , $t = 8.447$, $P = 0.0011$; day 5: 0.6890 ± 0.0070 vs. 0.5520 ± 0.0118 , $t = 17.310$, $P < 0.0001$; day 6: $0.7320 \pm$

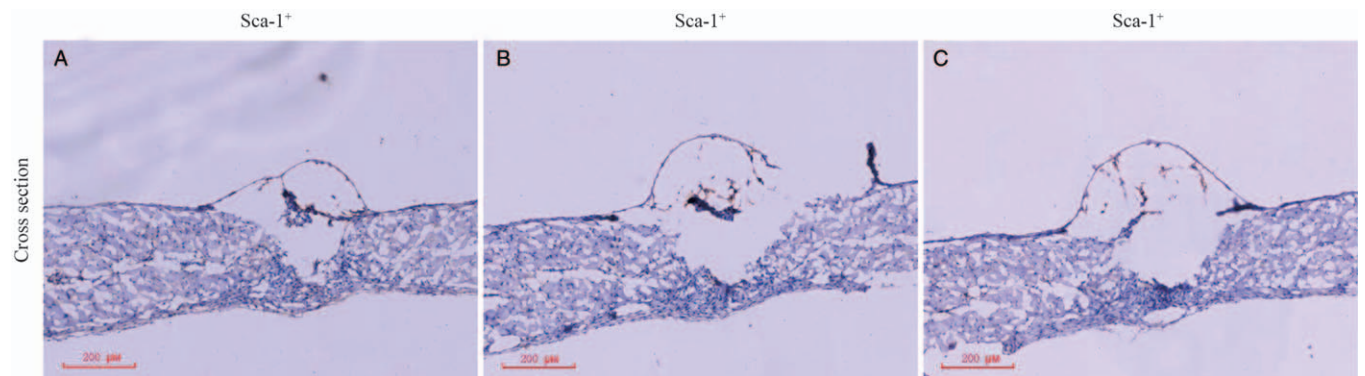


Figure 2: Sca-1 immunohistochemical staining of the CV8 acupoint tissues in mice. (A-C) Immunohistochemical staining showed that Sca-1-positive cells were distributed in the multi-layered slices of CV8 acupoint tissues. CV8: Shenque; Sca-1: Stem cell antigen-1.

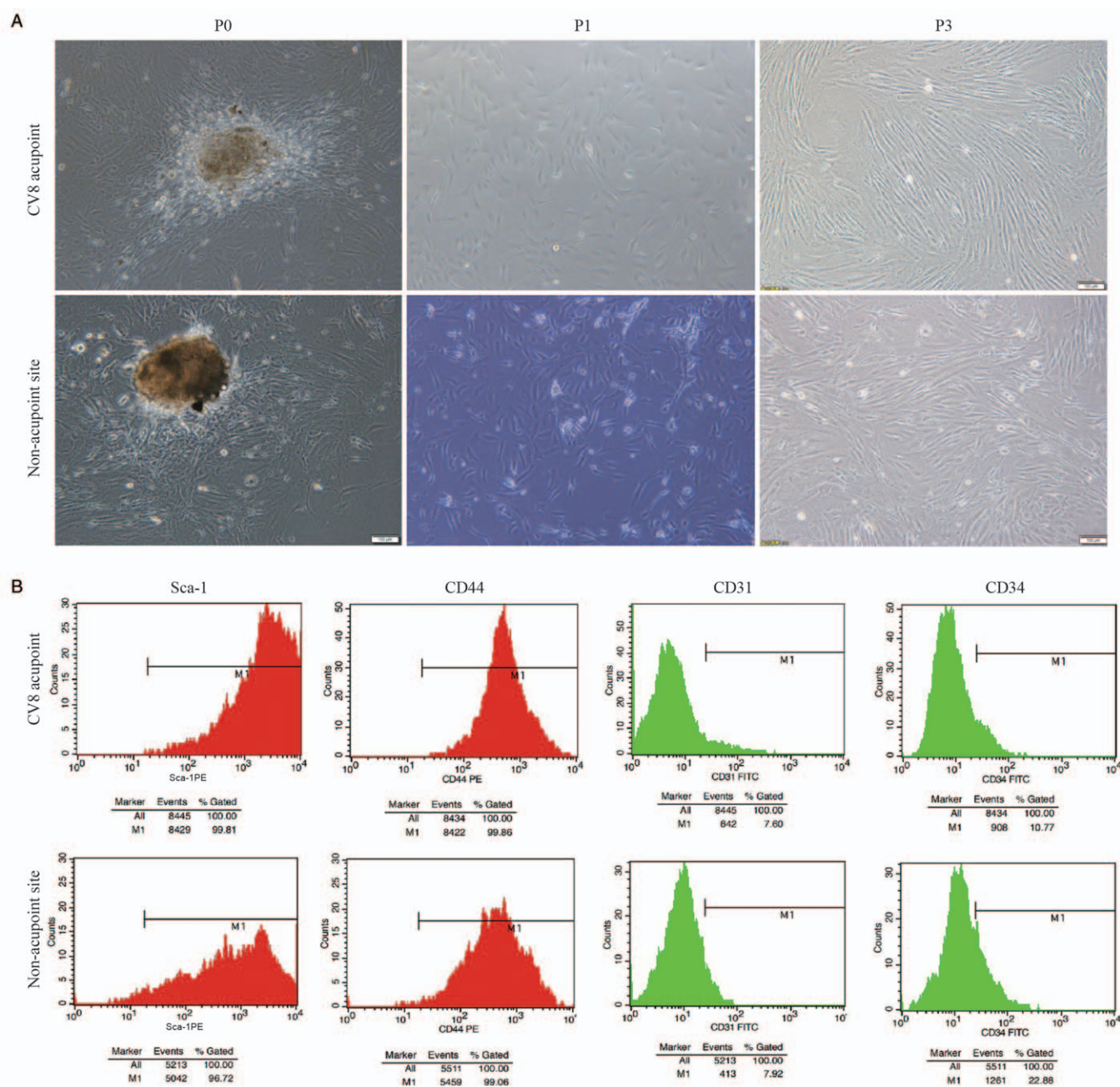


Figure 3: Identification of the morphology and immunophenotype of somatic stem cells from the CV8 acupoint and groin non-acupoint. (A) The P0, P1, and P3 cells of both groups showed the similar morphological characteristics and the P3 cells of both groups were observed to have a similar long fusiform and fibroblast-like morphology. (B) The somatic stem cells from both groups had high expression of stem cell markers, Sca-1 (99.81% vs. 96.72%) and CD44 (99.86% vs. 99.06%), and low expression of CD31 (7.60% vs. 7.92%) and CD34 (10.77% vs. 22.88%). CV8: Shenque; P0: The primary cells; P1: The first passage somatic stem cells; P3: The third passage somatic stem cells; Sca-1: Stem cell antigen-1.

0.0090 vs. 0.6157 ± 0.0123 , $t = 13.190$, $P = 0.0002$; and day 7: 0.7550 ± 0.0050 vs. 0.6313 ± 0.0051 , $t = 42.560$, $P < 0.0001$ [Figure 4].

Somatic stem cells from the CV8 acupoint have greater adipogenic and neurogenic stem cell-like cell differentiation ability and weaker osteogenic ability compared with the non-acupoint

In adipogenic induction, all cells were gradually changed from fusiform to the round shape, observed in lipid droplets found in the cytoplasm of some cells by Oil Red O

staining. After further induction, the quantity and size of lipid droplets were increased and fused gradually in the cytoplasm, suggesting that adipogenic differentiation occurred in cells from both groups. In contrast, non-induced controls lacked lipid droplets formation [Figure 5A]. Based on statistical results, the percentage of Oil Red O staining area in induced CV8 acupoint and non-acupoint sites were $(9.224 \pm 0.345)\%$ vs. $(3.933 \pm 1.800)\%$, respectively. The difference between the two groups was statistically significant ($t = 5.000$, $P = 0.0075$; Figure 5B), which indicated that the adipogenic differentiation ability of somatic stem cells at the

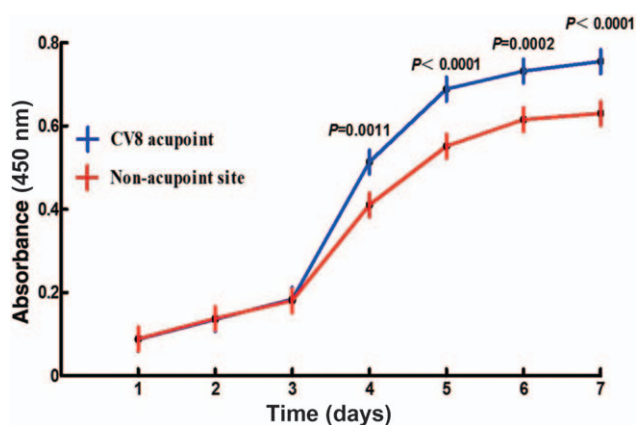


Figure 4: Comparison of proliferation ability of somatic stem cells from CV8 acupoint and non-acupoint site. The growth curve indicated that the somatic stem cells from the CV8 acupoint had better proliferation activity than the non-acupoint site. A: Absorbance; CV8: Shenque.

CV8 acupoint was greater than non-acupoint. Similar trends were also observed in neurogenic stem cell-like cell differentiation. After 1 week of induction, the cells clumped into “balls” and immunofluorescence staining results suggested that nestin-positive neurospheres were present in both induced groups. However, there were no obvious neurospheres in non-induced groups [Figure 5C]. The number of neurospheres was significantly more in the induced CV8 acupoint than the non-acupoint site (diameter $<50\ \mu\text{m}$: 7.2000 ± 1.3040 vs. 2.6000 ± 0.5477 , $t = 7.273$, $P < 0.0001$; diameter $50\text{--}100\ \mu\text{m}$: 2.6000 ± 0.5477 vs. 1.0000 ± 0.7071 , $t = 4.000$, $P = 0.0039$; and diameter $>100\ \mu\text{m}$: 2.6000 ± 0.5477 vs. 0.8000 ± 0.8367 , $t = 4.025$, $P = 0.0038$). These results indicated that the ability to differentiate into neurogenic stem cell-like cells in the CV8 acupoint was greater [Figure 5D]. However, osteogenic differentiation of somatic stem cells was lower in the CV8 acupoint than that in non-acupoint, which was indicated by Alizarin Red S staining. In contrast, there was no obvious mineralization found in both non-induced groups [Figure 5E]. The statistical results showed that the percentage of mineralization area was $(2.697 \pm 0.627)\%$ vs. $(7.254 \pm 0.958)\%$ in the induced CV8 acupoint and non-acupoint site groups, respectively. The difference between the two groups was statistically significant ($t = 6.893$, $P = 0.0023$; Figure 5F).

Discussion

In TCM, “navel therapy” plays important roles in gastrointestinal regulation and qi and blood supplementation.^[14-16] Moxibustion, acupuncture, and drug application at the navel have been applied for more than 2000 years in TCM. In recent years, clinical applications of navel therapy have been cooperating with internal medicine, surgery, gynecology, pediatrics, and dermatology.^[17-19] Scientific evidence for the exact mechanism of the navel therapy in treating diseases is still hidden and required to be explored. Our experimental results demonstrated that adipose tissues at the CV8 acupoint are rich in somatic stem cells that exhibit acupoint specificity when compared to stem cells from non-acupoint sites. Practitioners of TCM

meridianology regard the meridian system to be a regulatory system. As an acupoint on the meridian, the CV8 acupoint elicits its effects through the conception and belt vessels. On the other hand, somatic stem cells possess migration capabilities and can migrate to corresponding lesion sites. Therefore, we hypothesized that the curative effect of the CV8 acupoint may be associated with somatic stem cell functions.

Previous morphological observations reported that skin at the site of CV8 acupoint is thin with no subcutaneous fats.^[11] However, our results for the first time showed that the CV8 acupoint in mice was rich in adipose tissues. After it is confirmed that bone marrow is the stem cell bank *in vivo*, adipose tissue is another abundant tissue source rich in stem cells. After Zuk *et al*^[20,21] isolated pluripotent stem cells from adipose tissues. Other research groups also have successfully isolated pluripotent stem cells from the subcutaneous fats in different experimental animals that have similar biological characteristics.^[22-25] These cells are termed as adipose-derived stem cells (ASCs) and are widely used as “seed cells” in tissue engineering for animal experiments. In this study, we observed that adipose cells at the linea alba of the CV8 acupoint showed a mass-like distribution. We further revealed that the somatic stem cells obtained from the adipose tissue of CV8 acupoint in mice showed adipogenic, osteogenic, and neurogenic stem cell-like cell differentiation tendency. Compared with the stem cells derived from adipose tissue of non-acupoint sites in the groin, the stem cells of CV8 acupoint had enhanced proliferation, adipogenic, and neurogenic stem cell-like cell differentiation potentials, and reduced osteogenic differentiation capacities. Currently, it is believed that adipose cells can secrete many regulatory factors that affect adipose cells and other tissue.^[26] In addition, some articles have reported that moxibustion at the CV8 acupoint is effective in up-regulating serum adiponectin content.^[27] Does a high adipogenic potential suggest that adipose tissue somatic stem cells derived from the CV8 acupoint stimulate microenvironmental changes in acupoints to differentiate into adipose cells and participate in the function of the CV8 acupoint? Of course, it needs to be further verified by *in vivo* experiments, which is the limitation of *in vitro* experiments.

In stem cell therapy, stem cells migrate into the corresponding lesion sites with enhanced proliferation through facilitating differentiation to repair tissues. For example, stem cell therapy showed significant efficacy in treating depression.^[28,29] According to our results, we speculated that significant efficacy in navel therapy might depend on the function of the CV8 acupoint somatic stem cells when receiving external stimulation. In addition, our results imply that a reasonable strategy to aim somatic stem cells at the CV8 acupoint might have a greater impact on navel therapy.

Funding

This study was supported by the National Natural Science Foundation Projects (No. 81671462), Shanxi Natural Science Foundation Projects (No. 201901D211315 and 201901D111184), and Science and Technology Development Program of Xinzhou (No. 20180103).

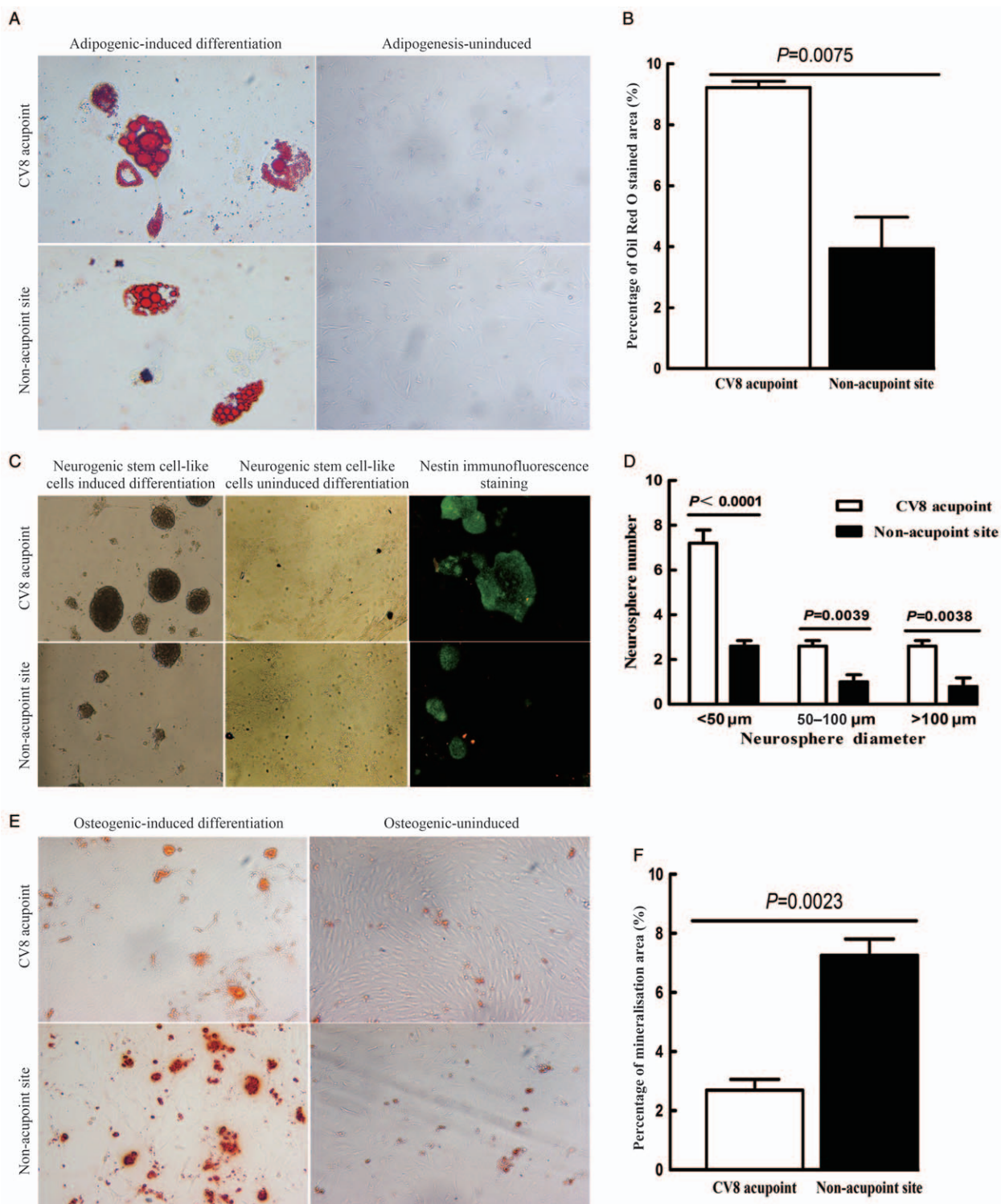


Figure 5: Comparison of adipogenic, neurogenic stem cell-like cell, and osteogenic differentiation abilities of both somatic stem cells from the CV8 acupoint and non-acupoint. (A) Compared with the non-induced group, the induced group showed positive staining for Oil Red O (original magnification $\times 400$). (B) Statistical analysis of adipogenic differentiation abilities of induced somatic stem cells from the CV8 acupoint and the non-acupoint site. (C) Compared with the non-induced group, the induced group showed the cells clumped into spherical clusters and grew in a suspension after 1 week (original magnification $\times 100$). The neurospheres that grew in a suspension showed positive nestin expression (immunofluorescence staining, original magnification $\times 200$). (D) Statistical analysis of neurogenic stem cell-like cell differentiation ability of induced somatic stem cells from the CV8 acupoint and the non-acupoint site. (E) Compared with the non-induced group, the induced group showed positive staining with Alizarin Red S (original magnification $\times 100$). (F) Statistical analysis of osteogenic differentiation abilities of induced somatic stem cells from the CV8 acupoint and the non-acupoint site. CV8: Shenque.

Conflicts of interest

None.

References

- Zhou W, Benharash P. Effects and mechanisms of acupuncture based on the principle of meridians. *J Acupunct Meridian Stud* 2014;7:190–193. doi: 10.1016/j.jams.2014.02.007.
- Croley TE. Acupuncture the past and the present. In: Hung KC, ed. *Acupuncture points-histological properties*. New York: Vantage Press; 1996:47.
- Zhang JS, Ma K, Geng LQ, Xing G. Progress studying on the specificity of acupoint. *China J Trad Chin Med Pharmacy* 2018;33:5045–5048. doi:CNKI:SUN:BXYY.0.2018-11-071.
- Sun ZH, Hu G, Zhao HY. Survey of study on acupoint morphology in recent years. *Chin Acup Moxib* 2002;21:64–65. doi:10.13703/j.0255-2930.2002.01.040.
- Ogay V, Kim MS, Seok HJ, Choi CJ, Soh KS. Catecholamine-storing cells at acupuncture points of rabbits. *J Acupunct Meridian Stud* 2008;1:83–90. doi: 10.1016/S2005-2901(09)60027-3.
- Hsiu H, Huang SM, Chao PT, Jan MY, Hsu TL, Wang WK, *et al*. Microcirculatory characteristics of acupuncture points obtained by laser Doppler flowmetry. *Physiol Meas* 2007;28:N77–N86. doi: 10.1088/0967-3334/28/10/N01.
- Ngai SPC, Jones AYM, Cheng EKW. Lung meridian acupuncture point skin impedance in asthma and description of a mathematical relationship with FEV1. *Respir Physiol Neurobiol* 2011;179:187–191. doi: 10.1016/j.resp.2011.08.004.
- She C, Xu DS, Cui JJ, Wang J, He W, Wang XY, *et al*. Our considerations about studies on structure of acupuncture points. *Zhen Ci Yan Jiu* 2018;43:285–289. doi: 10.13702/j.1000-0607.170911.
- Li SQ, Zhang XN, Ma FJ, Sun MS, Gao SZ, Ma YX. Effect of umbilical therapy on mast cells in shenque acupoint of rats with cold coagulation and blood stasis dysmenorrhea. *Lishizhen Med Materia Medica Res* 2017;28:2288–2290. doi: CNKI:SUN:SZGY.0.2017-09-089.
- Sui PS, Liu CM, Yu YP, Ma YX. Effect of medicine moxibustion with navel on mast cells in shenque point of rats with diarrhea-predominant irritable bowel syndrome. *Zhejiang J Trad Chin Med* 2015;50:649–650. doi: 10.13633/j.cnki.zjtc.2015.09.017.
- Jiang J, Xu W, Yu X, Wu X. Analysis of specificity of Shenque (CV8) based on vascular biology. *Chin Acup Moxib* 2017;37:1304–1308. doi: 10.13703/j.0255-2930.2017.12.014.
- Gurusamy N, Alsayari A, Rajasingh S, Rajasingh J. Adult stem cells for regenerative therapy. *Prog Mol Biol Transl Sci* 2018;160:1–22. doi: 10.1016/bs.pmbts.2018.07.009.
- Hu YL, Liu ZJ. *Manual of acupuncture techniques for small animals*. Beijing: Chemical Industry Press; 2009:204.
- Li H, Zhou Y, Li Z, Zhu L, Xiong JW, Li YT, *et al*. Clinical observation on umbilical moxibustion therapy treating 30 cases of diarrhea type irritable bowel syndrome with stagnation of liver Qi and spleen deficiency. *J Trad Chin Med* 2018;59:2034–2036. doi:10.13288/j.11-2166/r.2018.23.014.
- Li B, Zhang Y, Yang QM. Umbilical moxibustion for patients with idiopathic pulmonary fibrosis complicated with gastroesophageal reflux of lung-spleen qi deficiency. *Chin Acup Moxib* 2019;39:241–245. doi: 10.13703/j.0255-2930.2019. 03. 004.
- Mao LL, Jin YP. Professor JINYa-pei's experience in the treatment of perimenopausal insomnia with navel acupuncture combined with body acupuncture. *Chin Acup Moxib* 2020;40:295–298. doi: 10.13703/j.0255-2930.20190407-0002.
- Zhang B, Chen YQ, Zhou CX, Chen RX. Technical elements and clinical application of umbilical refining of heat-sensitive moxibustion. *Chin Acup Moxib* 2020;40:965–967. doi: 10.13703/j.0255-2930.20191214-k0006.
- Liu XZ, Zeng Z. Umbilical therapy combined with moxibustion for autumn diarrhea in children. *Chin Acup Moxib* 2019;39:832–836. doi: 10.13703/j.0255-2930.2019.08.009.
- Chen PB, Qi SS, Cui J, Yang XF, Chen J, Wang XG, *et al*. Herbal-cake-partitioned moxibustion of “Shenque” (CV8) has a relative specific effect in relieving abdominal pain and in regulating neuroendocrine-immune network in primary dysmenorrhea rats. *Zhen Ci Yan Jiu* 2019;44:120–124. doi: 10.13702/j.1000-0607.170811.
- Zuk PA, Zhu M, Mizuno H, Huang J, Futrell JW, Katz AJ, *et al*. Multilineage cells from human adipose tissue: implications for cell-based therapies. *Tissue Eng* 2001;7:211–228. doi: 10.1089/107632701300062859.
- Zuk PA, Zhu M, Ashjian P, De Ugarte DA, Huang JI, Mizuno H, *et al*. Human adipose tissue is a source of multipotent stem cells. *Mol Biol Cell* 2002;13:4279–4295. doi: 10.1091/mbc.e02-02-0105.
- Cousin B, Andre M, Arnaud E, Penicaud L, Casteilla L. Reconstitution of lethally irradiated mice by cells isolated from adipose tissue. *Biochem Biophys Res Commun* 2003;301:1016–1022. doi: 10.1016/S0006-291X(03)00061-5.
- Ogawa R, Mizuno H, Watanabe A, Migita M, Hyakusoku H, Shimada T. Adipogenic differentiation by adipose-derived stem cells harvested from GFP transgenic mice-including relationship of sex differences. *Biochem Biophys Res Commun* 2004;319:511–517. doi: 10.1016/j.bbrc.2004.05.021.
- Ong WK, Tan CS, Chan KL, Goesantoso GG, Chan XHD, Chan E, *et al*. Identification of specific cell-surface markers of adipose-derived stem cells from subcutaneous and visceral fat depots. *Stem Cell Rep* 2014;2:171–179. doi: 10.1016/j.stemcr.2014.01.002.
- Safford KM, Hicok KC, Safford SD, Halvorsen YD, Wilkison WO, Gimble JM, *et al*. Neurogenic differentiation of murine and human adipose-derived stromal cells. *Biochem Biophys Res Commun* 2002;294:371–379. doi: 10.1016/S0006-291X(02)00469-2.
- Funcke JB, Scherer PE. Beyond adiponectin and leptin: adipose tissue-derived mediators of inter-organ communication. *J Lipid Res* 2019;60:1648–1684. doi: 10.1194/jlr.R094060.
- Zhao CJ, Huang YZ, Jiang YF, Lu MJ. Effect of moxibustion at “Shenque” (CV8) and “Zusanli” (ST36) on expression of adiponectin and adiponectin receptor in Alzheimer's disease rats. *Zhen Ci Yan Jiu* 2019;44:419–423. doi: 10.13702/j.1000-0607.180464.
- Hattiangady B, Shetty AK. Neural stem cell grafting counteracts hippocampal injury-mediated impairments in mood, memory, and neurogenesis. *Stem Cells Transl Med* 2012;1:696–708. doi: 10.5966/sctm.2012-0050.
- Huang Y, Li Y, Chen J, Zhou H, Tan S. Electrical stimulation elicits neural stem cells activation: new perspectives in CNS repair. *Front Hum Neurosci* 2015;9:586. doi: 10.3389/fnhum.2015.00586.

How to cite this article: Hao YH, Liu ZZ, Zhao H, Wang L, Khan A, Mu JB, Wang YF, Yang LH, Zhou R, Xie J. Identification and characterization of murine adipose tissue-derived somatic stem cells of Shenque (CV8) acupoint. *Chin Med J* 2021;134:2730–2737. doi: 10.1097/CM9.0000000000001850